# Supplemental Material

# Dynamic Aggregation of Poly-N-Isopropylacrylamide Characterized by Second-Order Scattering

Luke A. Fulton[1], Pei Zhang[2], W. Rudolf Seitz[1], John G. Tsavalas[1,2]*, Roy P. Planalp[1]*

[1]Department of Chemistry, University of New Hampshire, Durham, New Hampshire 03824, United States

[2]Materials Science Program, University of New Hampshire, Durham, New Hampshire 03824, United States

## Table of Contents



## $^1$H-NMR Spectra

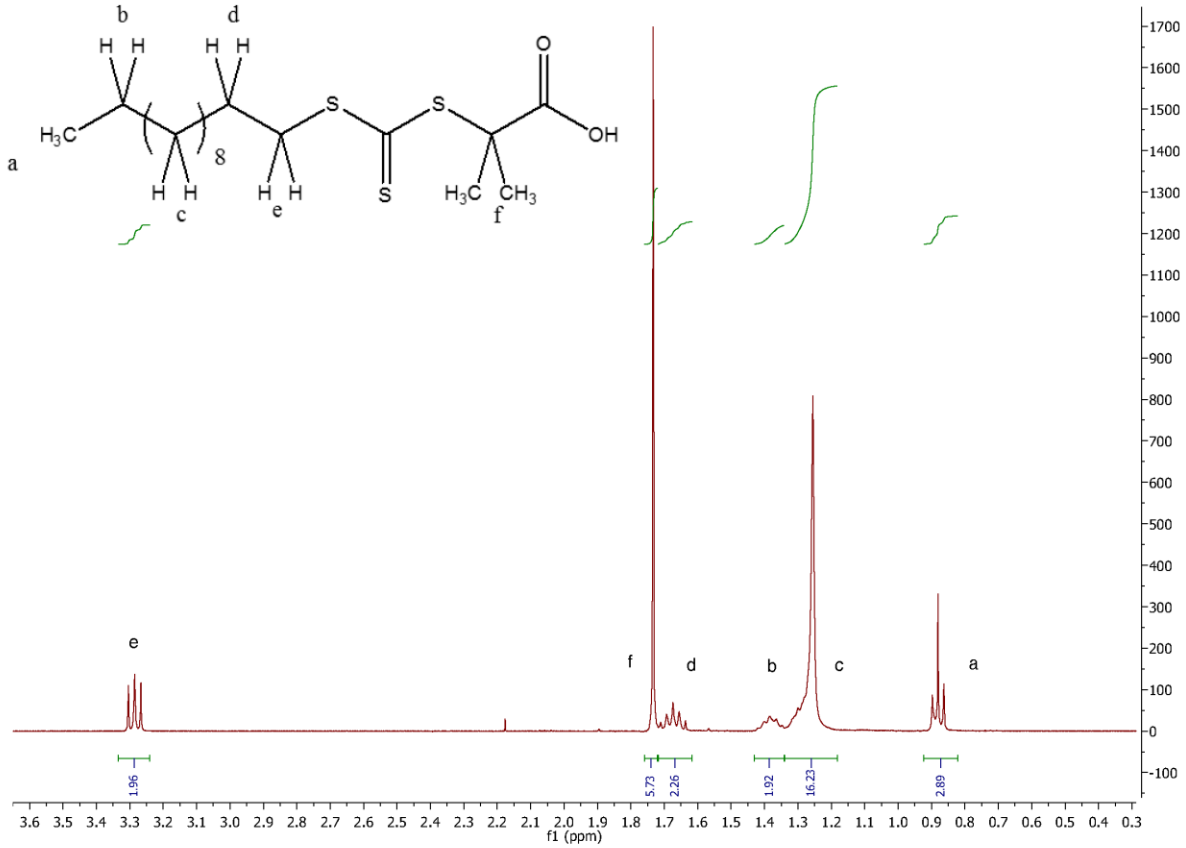


Figure S1. $^{1}$H NMR of chain transfer agent 2-(dodecylthiocarbonothioylthio)-2-methylpropionic

acid in $CDCl_3$. 400 MHz 32 scans.

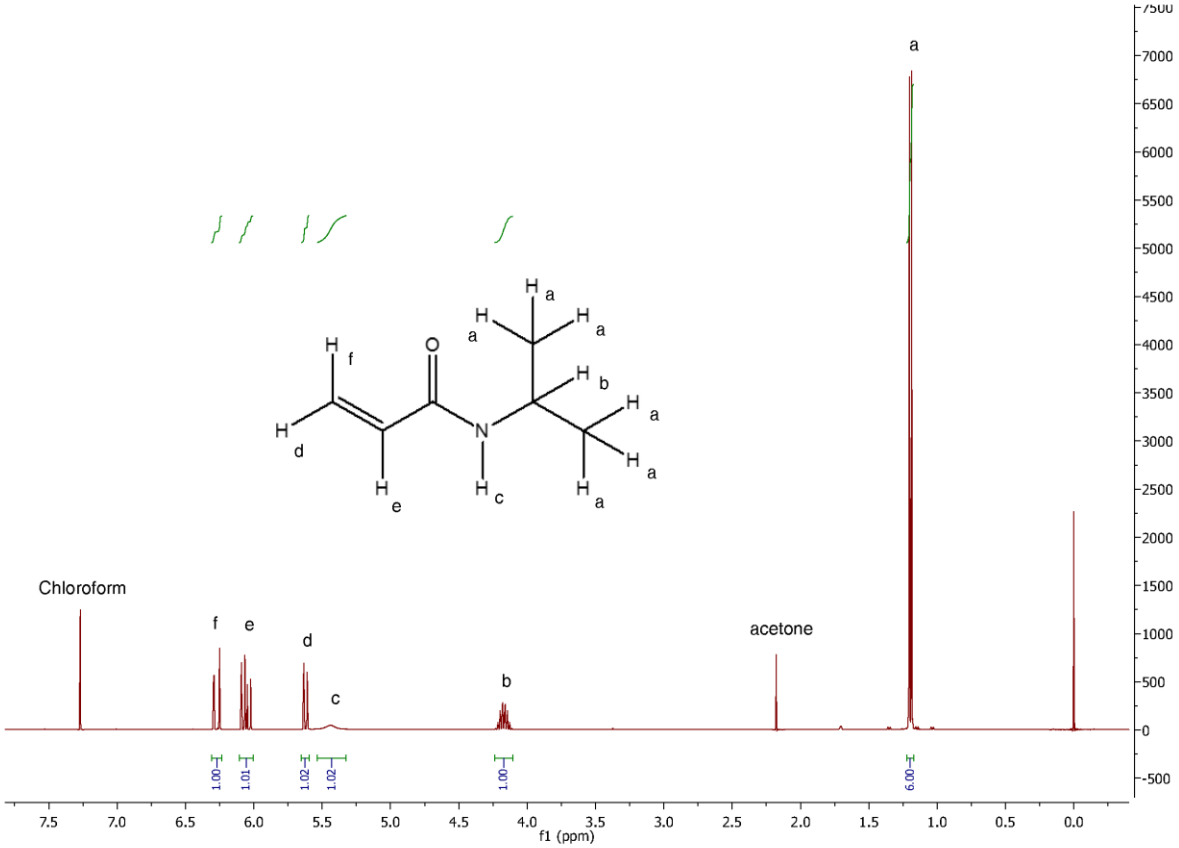


Figure S2. $^1$H NMR of *n*-isopropylacrlyamide monomer unit in $CDCl_3$. 400 MHz 32 scans.

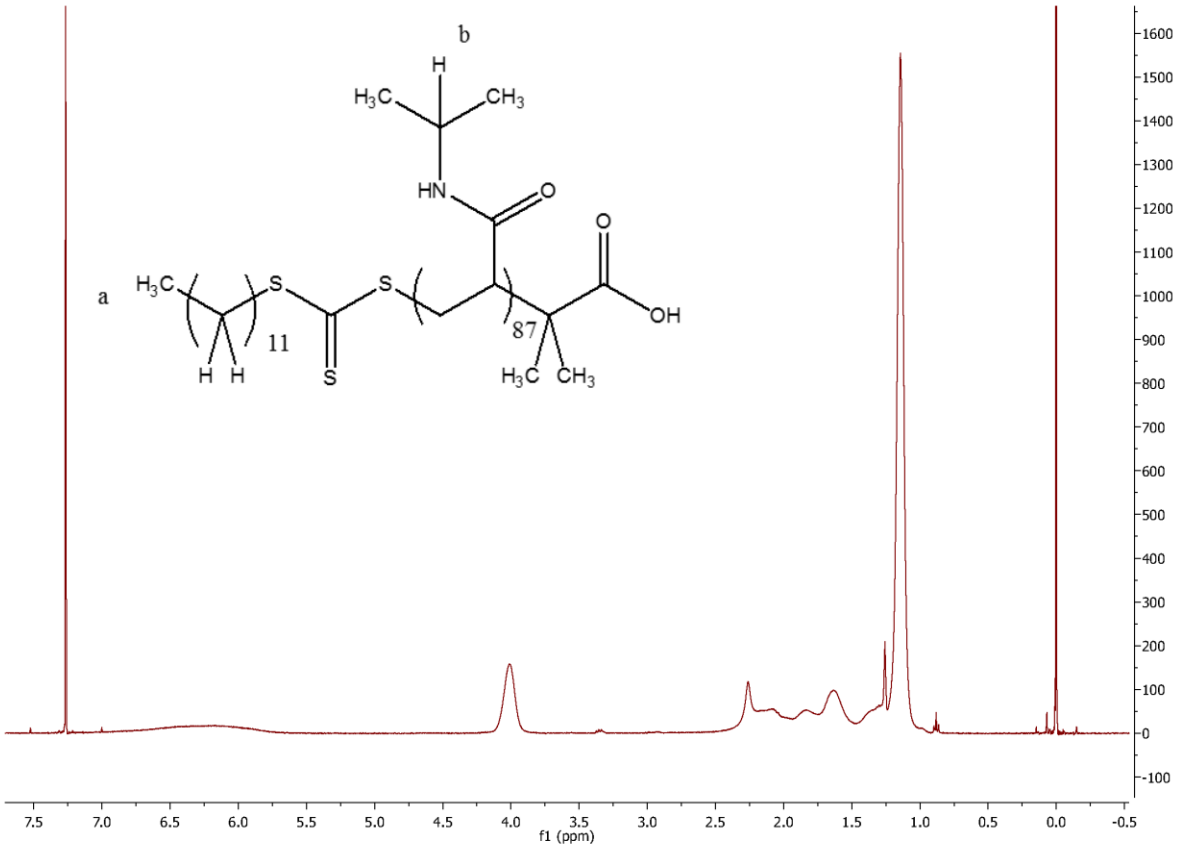
b
a
11
87
OH
f1 (ppm)

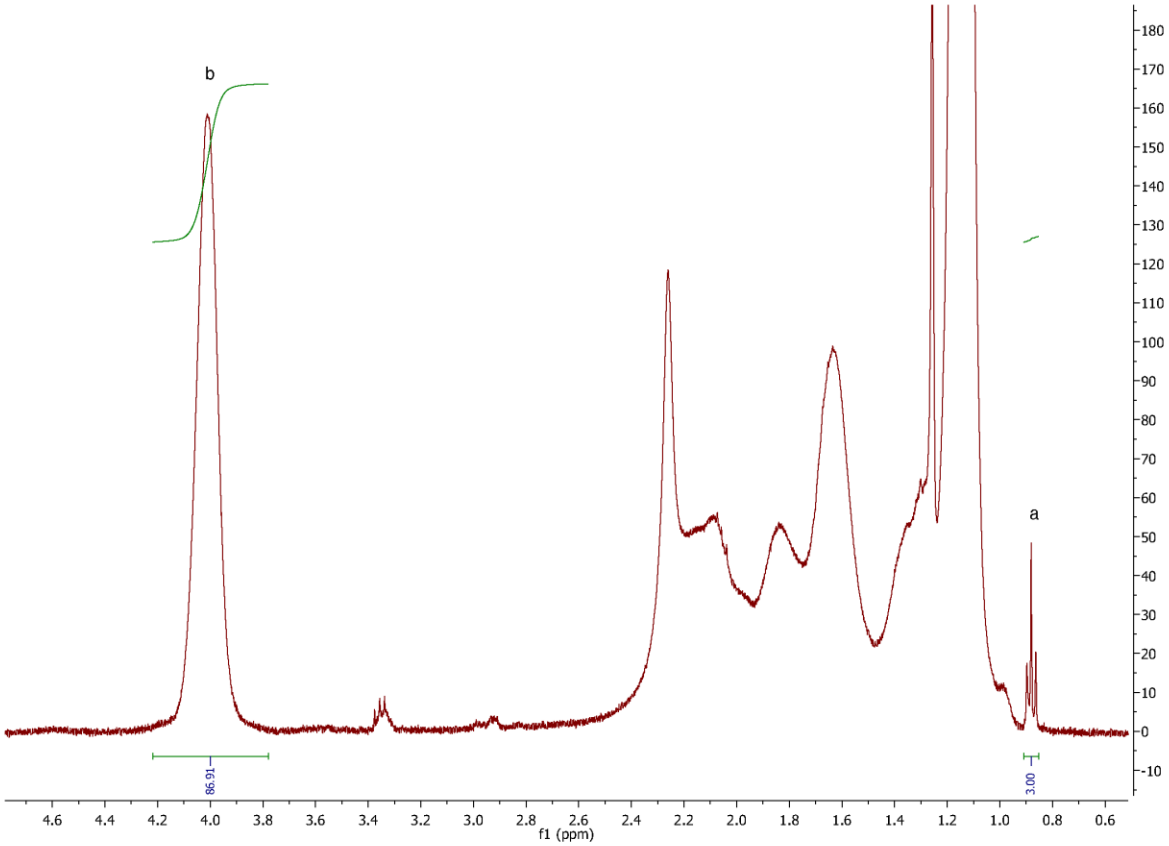


Figure S3. $^{1}H$ NMR of prepared PNIPAM in $CDCl_3$, 400 MHz 300 scans. Full spectra shown above, zoom with relevant integrations shown below, calculated $M_n$ of 10,200.

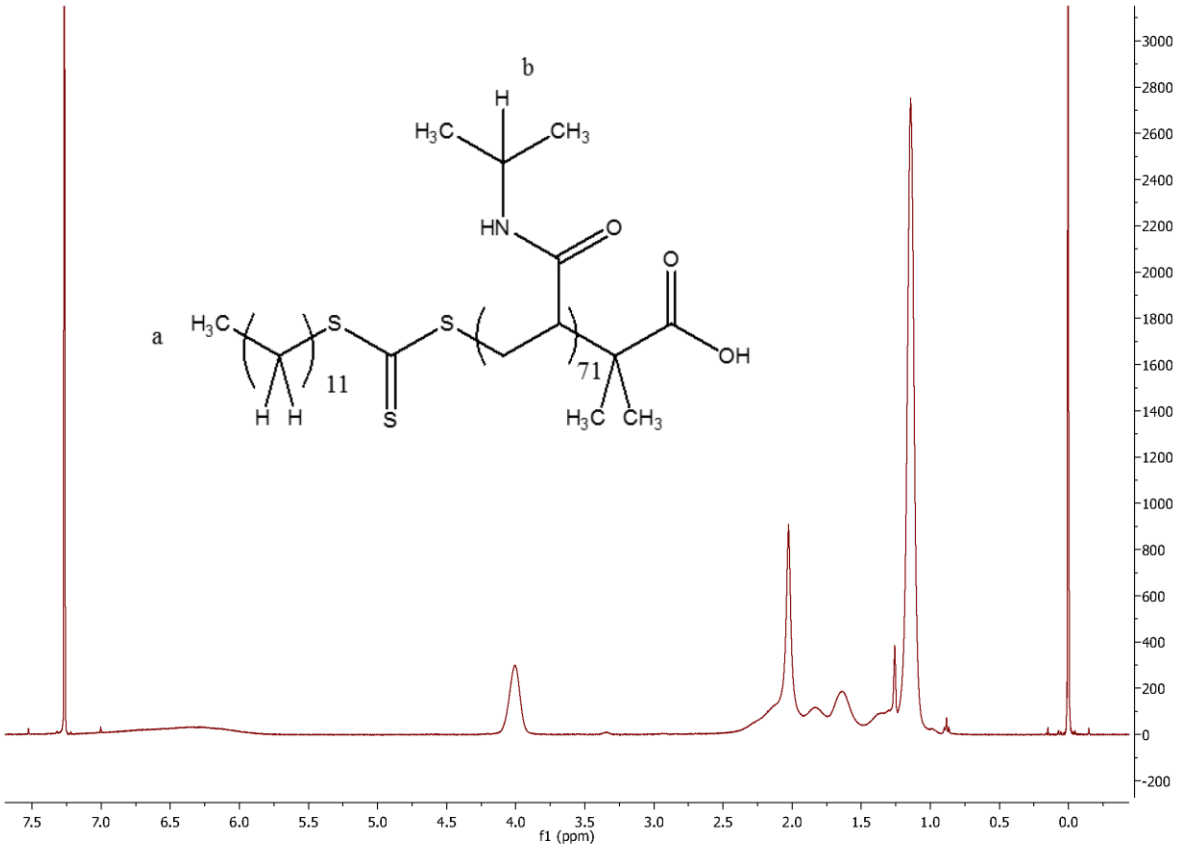
b
a
11
71
OH
f1 (ppm)

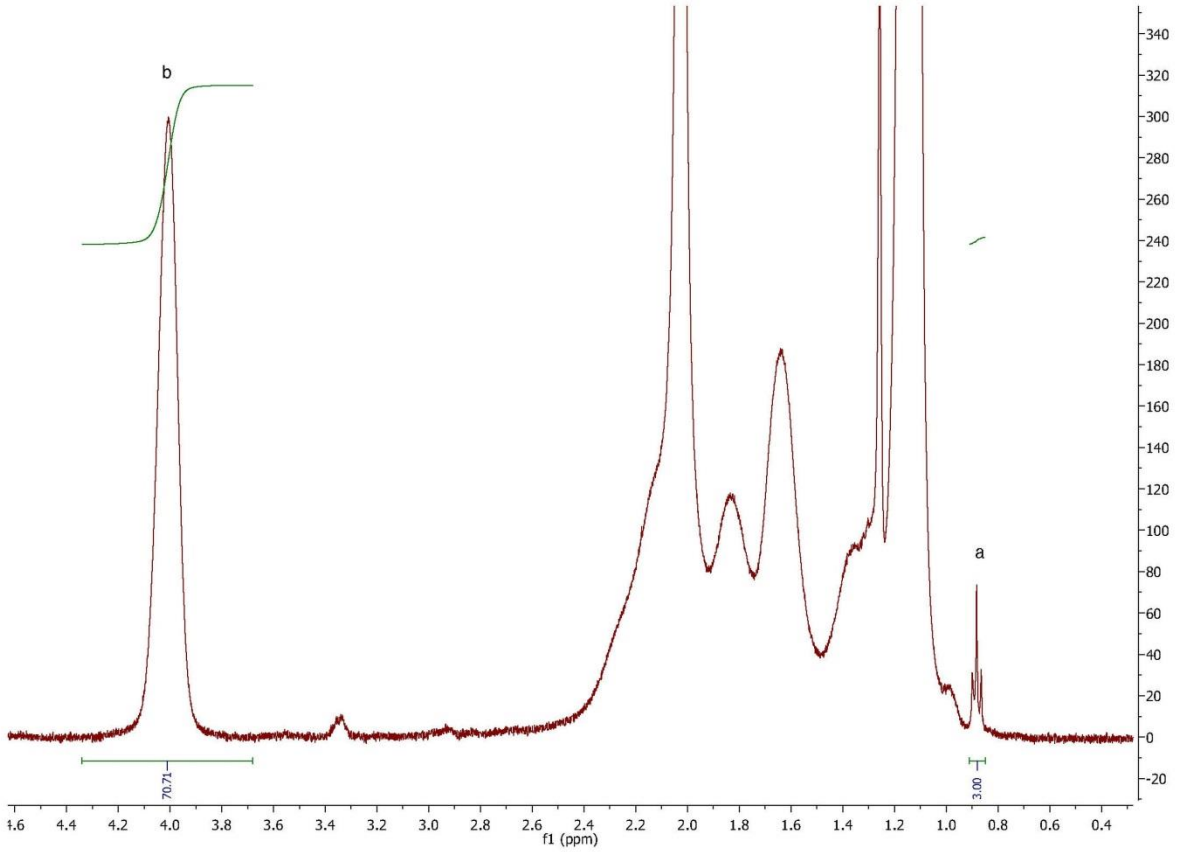


Figure S4. $^{1}H$ NMR of prepared PNIPAM in $CDCl_3$, 400 MHz 300 scans. Full spectra shown above, zoom with relevant integrations shown below, calculated $M_n$ of 8400.

## Experimental

### Sample Preparation

Polystyrene samples were diluted to 0.05 mg/mL synthesized stock solutions using ultra-pure water to give partially turbid suspensions. Stock solutions of PNIPAm, MES buffer, MOPS buffer, $Cu(NO_3)_2$, and $Zn(NO_3)_2$ were each prepared by dissolving the solid compound in ultra-pure water. Buffer solutions were tuned to pH 6.3 with prepared NaOH solution. PNIPAm samples were prepared using aliquots of polymer, buffer, metal salt, and additional ultra-pure water as necessary to achieve 0.05 mg/mL PNIPAm, 0.1 M pH 6.3 buffer, and chosen metal concentration. Solutions were mixed thoroughly prior to gathering scattering measurements. PNIPAm samples appeared as clear colorless solutions prior to heating and slightly turbid suspensions after heating

**Second Order Scattering Methods**

Scattering was measured on a Cary Eclipse Fluorescence Spectrophotometer using a 1 cm pathlength glass fluorescence cell. Excitation and Emission slit widths were 5 nm. Excitation filter was set to "auto" and the Emission filter set to "open". PMT detector voltage was 600 V. Emission wavelengths are always set to double the chosen excitation wavelength; 375 nm emission and 750 nm emission, 400 nm emission and 800 nm emission, 425 nm emission and 850 nm emission, 450 nm emission and 900 nm emission. intensity readings were collected at 0.1 second intervals. Raw data was averaged over 10 second intervals before use in SOS prediction model calculations.

**Dynamic Light Scattering Methods**

We found that using 0.45 μm pvdf Acrodisc syringe filters partially removed polymer, which rendered the final concentration of 0.05 mg/mL samples too low to observe. To reduce interference from dust particles, stock solution volumes were instead prepared with ultra-pure water suction filtered through 0.2 μm polycarbonate membrane. All necessary glassware was prewashed with filtered water and kept upended prior to use to discourage dust collection. Even so, particle contamination remained a persistent difficulty which contributed to measured values. The impact on measured dispersity necessitated use of the "mean peak intensity size" rather than the preferred "Z-average diameter" for 0.05 mg/mL PNIPAM samples. Individual measurements with a PDI > 0.25, which in our samples indicated a broad dispersity index arising from contributions from contaminants, were rejected.

Fixed temperature experiments for phase transition and aggregation consisted of 180 consecutive collections of a single 20 second run. Sample volume of approx. 1 mL was placed from room temperature into the preheated 35 °C sample holder and collection initiated. A system optimization step occurs prior to the first collection which lasts for approximately one minute. Variable temperature experiments measured at 0.5 °C increments from 27 °C to 50 °C. At each increment temperature was allowed to equilibrate for 600 seconds before 3 measurements consisting of four runs lasting 20 seconds each with a 0 second delay were taken.

## Concentration Behavior

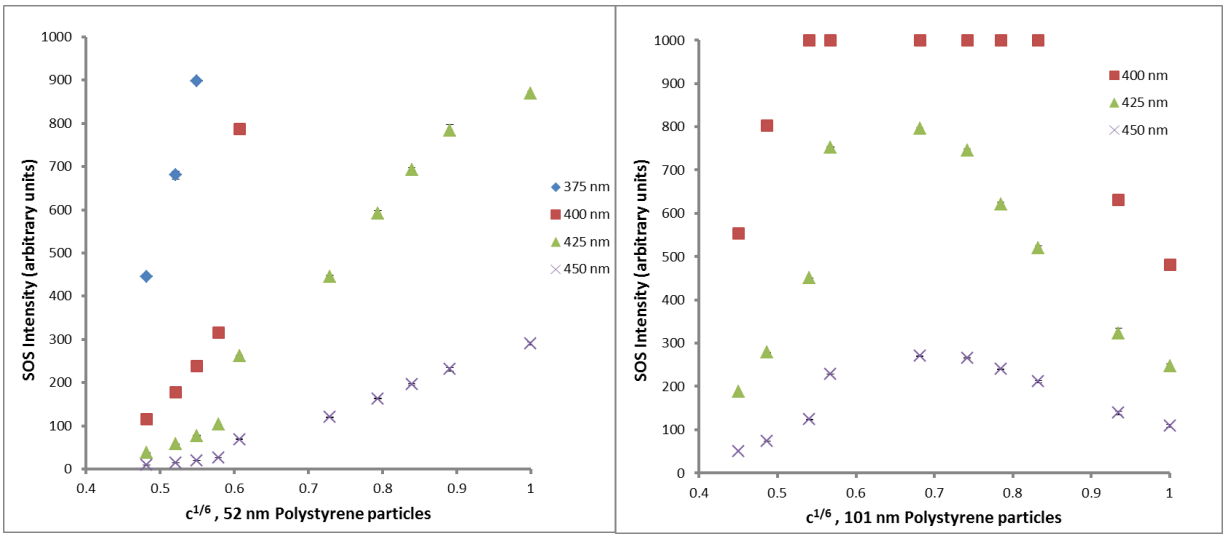


Figure S5. SOS intensities versus $c^{1/6}$ ranging from 0.224 mg/mL to 1.79 mg/mL for 52 nm particles (left) and 0.0495 mg/mL to 5.94 mg/mL for 101 nm particles (right). Legend displays excitation wavelengths. The relative concentration, c, is defined as a fraction compared to the highest concentration used. The highest value is by definition "1".

At low concentrations SOS intensity increases linearly with c1/6. Naked eye inspection easily observes that total scattering increases with polymer concentration. However, this trend is not mimicked by the measured SOS intensities. Instead, intensity initially increases with polymer concentration before changing behavior to intensity decreasing with additional polymer. This shift in behavior is first observed at 1.39 mg/mL for 101 nm polystyrene particles. Because no evidence was found for particle settling or precipitation, we concluded that this behavior arose from an inner filter effect. As the high amount of scattering diminishes the intensity of incident light traveling through the sample, I0 goes down, the observable region within the sample receives less light with which to scatter. Subsequently, the instrument measures less SOS intensity despite the high amount of scattering occurring in the sample.

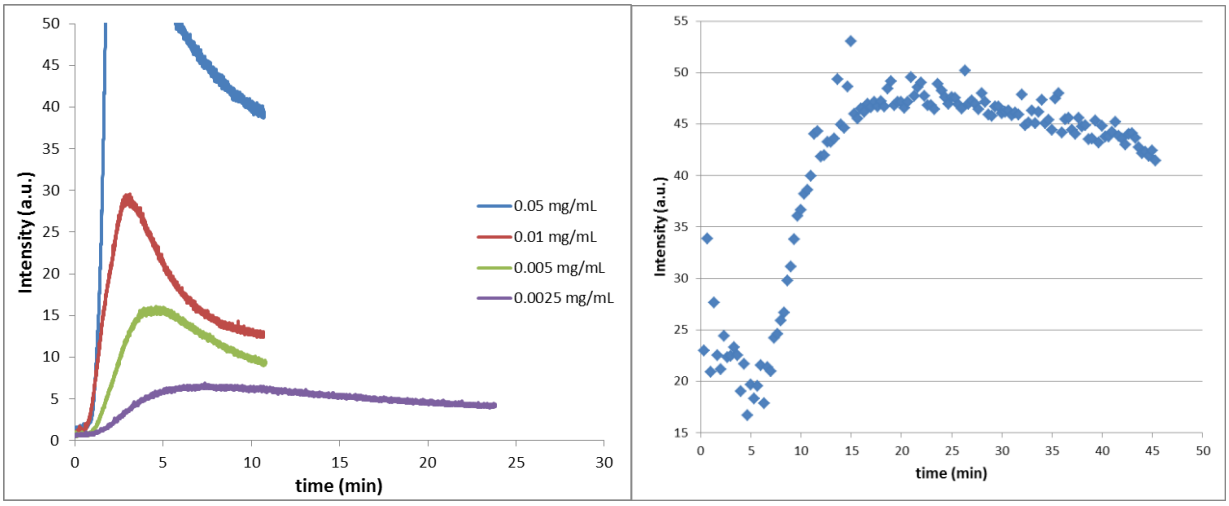


Figure S6. SOS scattering intensities at varying polymer concentration (left), First Order Scattering intensity at 0.001 mg/mL PNIPAm with 20s signal averaging (right). 8.4k Mn PNIPAm, 0.1 M MES buffer pH 6.3, 0.025 M $Zn(NO_3)_2$, 400 nm excitation. The increase, peak, and decrease in intensity measurements indicate that all concentrations shown are suitable for size calculations using the presented method.

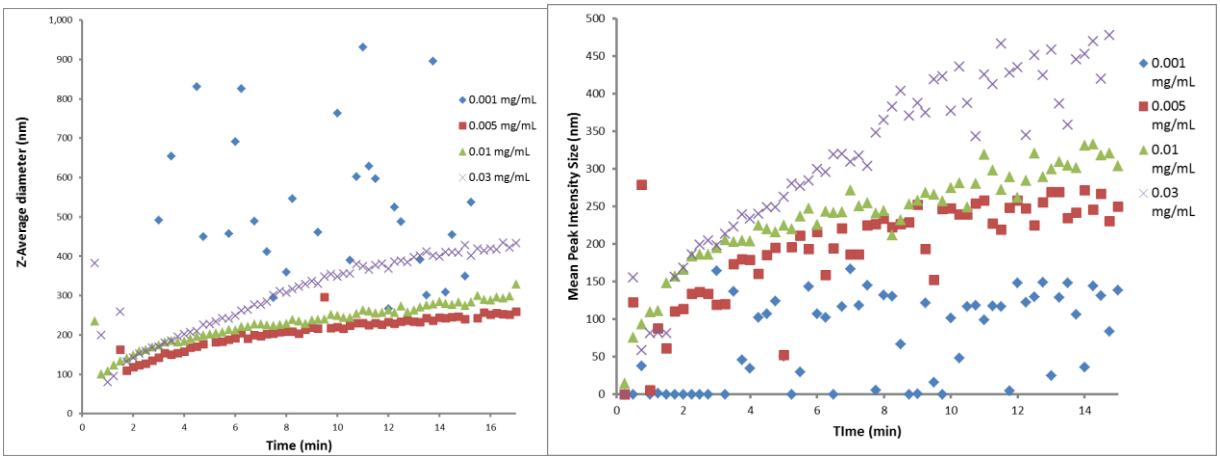


Figure S7. DLS measurements at varying polymer concentration. 8.4k $M_n$ PNIPAm, 0.1 M MES buffer pH 6.3, 0.025 M $Zn(NO_3)_2$. The erratic behavior at 0.001 mg/mL indicates that the concentration is too low for reliable analysis.

## Prediction Model Tables

What follows are the calculated values used to generate predictive models at different wavelength and refractive index. The predicted curve was assembled as a series of linear regressions between each data point (*x*=size and *y*= normalized K*I*c^(1/6)). Experimental data was treated using these regressions to convert $I/I_{max}$ into particle size.

**Table S1. Predictive model using 400 nm wavelength and 1.378 refractive index.**

| size | Ksc | I(theta) | c | K*I(theta)*c^(1/6) | normalized K*I*c^(1/6) |
|---|---|---|---|---|---|
| 10 | 1.81E-07 | 0.001852 | 0.00191 | 1.17908E-10 | 0.000245073 |
| 20 | 2.86E-06 | 0.001852 | 0.000239 | 1.31826E-09 | 0.00274002 |
| 30 | 1.42E-05 | 0.001851 | 7.07E-05 | 5.34038E-09 | 0.011100077 |
| 40 | 4.36E-05 | 0.001849 | 2.98E-05 | 1.42077E-08 | 0.029530974 |
| 50 | 0.000103 | 0.001846 | 1.53E-05 | 2.98824E-08 | 0.06211107 |
| 60 | 0.000204 | 0.001839 | 8.84E-06 | 5.39767E-08 | 0.112191553 |
| 70 | 0.000359 | 0.001828 | 5.57E-06 | 8.74606E-08 | 0.181788329 |
| 80 | 0.000578 | 0.001811 | 3.73E-06 | 1.30428E-07 | 0.271096297 |
| 90 | 0.000868 | 0.001785 | 2.62E-06 | 1.81901E-07 | 0.378084876 |
| 100 | 0.001231 | 0.001749 | 1.91E-06 | 2.39708E-07 | 0.498237027 |
| 110 | 0.001666 | 0.001699 | 1.43E-06 | 3.00606E-07 | 0.624815569 |
| 120 | 0.002169 | 0.001633 | 1.11E-06 | 3.60105E-07 | 0.748484887 |
| 130 | 0.002734 | 0.001546 | 8.69E-07 | 4.13045E-07 | 0.858521245 |
| 140 | 0.003354 | 0.001437 | 6.96E-07 | 4.53856E-07 | 0.943348273 |
| 150 | 0.004023 | 0.001305 | 5.66E-07 | 4.7763E-07 | 0.992762637 |
| 160 | 0.004737 | 0.001153 | 4.66E-07 | 4.81112E-07 | 1 |
| 170 | 0.005494 | 0.000988 | 3.89E-07 | 4.63697E-07 | 0.963802481 |
| 180 | 0.0063 | 0.000819 | 3.27E-07 | 4.28253E-07 | 0.890131785 |
| 190 | 0.00716 | 0.000657 | 2.78E-07 | 3.80309E-07 | 0.790477899 |
| 200 | 0.008084 | 0.000512 | 2.39E-07 | 3.26257E-07 | 0.678130803 |
| 210 | 0.009081 | 0.000389 | 2.06E-07 | 2.7156E-07 | 0.564441441 |
| 220 | 0.010161 | 0.000288 | 1.79E-07 | 2.19893E-07 | 0.457050572 |
| 230 | 0.011329 | 0.000208 | 1.57E-07 | 1.73383E-07 | 0.360379287 |
| 240 | 0.012588 | 0.000147 | 1.38E-07 | 1.33285E-07 | 0.277034976 |
| 250 | 0.013936 | 0.000103 | 1.22E-07 | 1.01189E-07 | 0.210322489 |

**Table S2. Predictive model using 400 nm wavelength and 1.45 refractive index.**

| size | Ksc | I(theta) | c | K*I(theta)*c^(1/6) | normalized K*I*c^(1/6) |
|---|---|---|---|---|---|
| 10 | 1.11E-06 | 0.001852 | 0.00191 | 7.22044E-10 | 0.000221183 |
| 20 | 1.75E-05 | 0.001852 | 0.000239 | 8.08716E-09 | 0.002477327 |
| 30 | 8.73E-05 | 0.001851 | 7.07E-05 | 3.28619E-08 | 0.010066545 |
| 40 | 0.000269 | 0.001849 | 2.98E-05 | 8.77563E-08 | 0.026882255 |

| | | | | | |
|---|---|---|---|---|---|
| 50 | 0.000638 | 0.001846 | 1.53E-05 | 1.85463E-07 | 0.056812496 |
| 60 | 0.001273 | 0.00184 | 8.84E-06 | 3.36804E-07 | 0.103172572 |
| 70 | 0.002254 | 0.001829 | 5.57E-06 | 5.48816E-07 | 0.168117962 |
| 80 | 0.003647 | 0.001812 | 3.73E-06 | 8.23045E-07 | 0.25212197 |
| 90 | 0.005497 | 0.001788 | 2.62E-06 | 1.15411E-06 | 0.353537235 |
| 100 | 0.007826 | 0.001754 | 1.91E-06 | 1.52898E-06 | 0.468371451 |
| 110 | 0.010625 | 0.001708 | 1.43E-06 | 1.92699E-06 | 0.590291062 |
| 120 | 0.013862 | 0.001647 | 1.11E-06 | 2.3209E-06 | 0.710958284 |
| 130 | 0.017488 | 0.001569 | 8.69E-07 | 2.68047E-06 | 0.821104209 |
| 140 | 0.021448 | 0.001473 | 6.96E-07 | 2.97351E-06 | 0.910871212 |
| 150 | 0.025702 | 0.001358 | 5.66E-07 | 3.17442E-06 | 0.972416277 |
| 160 | 0.030232 | 0.001226 | 4.66E-07 | 3.26447E-06 | 1 |
| 170 | 0.035055 | 0.001081 | 3.89E-07 | 3.23637E-06 | 0.991391545 |
| 180 | 0.04022 | 0.000927 | 3.27E-07 | 3.09435E-06 | 0.947886834 |
| 190 | 0.045807 | 0.000771 | 2.78E-07 | 2.85386E-06 | 0.874219735 |
| 200 | 0.051903 | 0.000621 | 2.39E-07 | 2.53792E-06 | 0.7774385 |
| 210 | 0.058589 | 0.000482 | 2.06E-07 | 2.17069E-06 | 0.664944629 |
| 220 | 0.065913 | 0.00036 | 1.79E-07 | 1.78021E-06 | 0.545329317 |
| 230 | 0.073879 | 0.000256 | 1.57E-07 | 1.39097E-06 | 0.42609403 |
| 240 | 0.082442 | 0.000173 | 1.38E-07 | 1.02318E-06 | 0.313429908 |
| 250 | 0.091516 | 0.000108 | 1.22E-07 | 6.97605E-07 | 0.213696136 |

**Table S3. Predictive model using 375 nm wavelength and 1.639 refractive index.**

| size | Ksc | I(theta) | c | K*I(theta)*c^(1/6) | normalized K*I*c^(1/6) |
|---|---|---|---|---|---|
| 10 | 8.91E-06 | 0.001852 | 0.00191 | 5.8129E-09 | 0.000268201 |
| 20 | 0.000142 | 0.001852 | 0.000239 | 6.53518E-08 | 0.003015262 |
| 30 | 0.00071 | 0.001851 | 7.07E-05 | 2.67105E-07 | 0.012323928 |
| 40 | 0.002207 | 0.001849 | 2.98E-05 | 7.18624E-07 | 0.033156545 |
| 50 | 0.005272 | 0.001844 | 1.53E-05 | 1.53106E-06 | 0.07064167 |
| 60 | 0.010618 | 0.001835 | 8.84E-06 | 2.8016E-06 | 0.129262682 |
| 70 | 0.01895 | 0.00182 | 5.57E-06 | 4.59241E-06 | 0.21188873 |
| 80 | 0.03084 | 0.001798 | 3.73E-06 | 6.90507E-06 | 0.31859276 |
| 90 | 0.046614 | 0.001764 | 2.62E-06 | 9.65709E-06 | 0.445567949 |
| 100 | 0.066258 | 0.001717 | 1.91E-06 | 1.26737E-05 | 0.584748688 |

| | | | | | |
|---|---|---|---|---|---|
| 110 | 0.089409 | 0.001652 | 1.43E-06 | 1.56831E-05 | 0.723601193 |
| 120 | 0.11547 | 0.001564 | 1.11E-06 | 1.83653E-05 | 0.847356059 |
| 130 | 0.14389 | 0.001451 | 8.69E-07 | 2.03981E-05 | 0.941145862 |
| 140 | 0.17442 | 0.001312 | 6.96E-07 | 2.15358E-05 | 0.993639845 |
| 150 | 0.20748 | 0.001149 | 5.66E-07 | 2.16737E-05 | 1 |
| 160 | 0.24409 | 0.000971 | 4.66E-07 | 2.08608E-05 | 0.962494323 |
| 170 | 0.2857 | 0.00079 | 3.89E-07 | 1.9293E-05 | 0.890158356 |
| 180 | 0.33351 | 0.000621 | 3.27E-07 | 1.7201E-05 | 0.793634042 |
| 190 | 0.38776 | 0.000473 | 2.78E-07 | 1.48279E-05 | 0.68414198 |
| 200 | 0.4473 | 0.000351 | 2.39E-07 | 1.23565E-05 | 0.570117466 |
| 210 | 0.50979 | 0.000253 | 2.06E-07 | 9.93058E-06 | 0.458186185 |
| 220 | 0.57261 | 0.000179 | 1.79E-07 | 7.68267E-06 | 0.354469951 |
| 230 | 0.63407 | 0.000124 | 1.57E-07 | 5.7607E-06 | 0.265792442 |
| 240 | 0.69416 | 8.71E-05 | 1.38E-07 | 4.34621E-06 | 0.200529358 |
| 250 | 0.75444 | 6.75E-05 | 1.22E-07 | 3.58737E-06 | 0.165517302 |

**Table S4. Predictive model using 400 nm wavelength and 1.628 refractive index.**

| size | Ksc | I(theta) | c | K*I(theta)*c^(1/6) | normalized K*I*c^(1/6) |
|---|---|---|---|---|---|
| 10 | 6.45E-06 | 0.001852 | 0.00191 | 4.20494E-09 | 0.000214271 |
| 20 | 0.000103 | 0.001852 | 0.000239 | 4.7301E-08 | 0.002410318 |
| 30 | 0.000514 | 0.001851 | 7.07E-05 | 1.93516E-07 | 0.009860972 |
| 40 | 0.001602 | 0.001849 | 2.98E-05 | 5.21699E-07 | 0.026584207 |
| 50 | 0.003835 | 0.001846 | 1.53E-05 | 1.11474E-06 | 0.056803789 |
| 60 | 0.007751 | 0.001839 | 8.84E-06 | 2.04944E-06 | 0.104433316 |
| 70 | 0.0139 | 0.001828 | 5.57E-06 | 3.38231E-06 | 0.172352225 |
| 80 | 0.022772 | 0.001811 | 3.73E-06 | 5.1345E-06 | 0.261638618 |
| 90 | 0.034717 | 0.001785 | 2.62E-06 | 7.27668E-06 | 0.370797884 |
| 100 | 0.049867 | 0.001749 | 1.91E-06 | 9.71436E-06 | 0.49501464 |
| 110 | 0.068105 | 0.001699 | 1.43E-06 | 1.22915E-05 | 0.626340576 |
| 120 | 0.089084 | 0.001633 | 1.11E-06 | 1.47907E-05 | 0.753691532 |
| 130 | 0.11233 | 0.001546 | 8.69E-07 | 1.69693E-05 | 0.864702961 |
| 140 | 0.13745 | 0.001437 | 6.96E-07 | 1.85983E-05 | 0.94771612 |
| 150 | 0.1643 | 0.001305 | 5.66E-07 | 1.95065E-05 | 0.993993111 |
| 160 | 0.1932 | 0.001153 | 4.66E-07 | 1.96244E-05 | 1 |

| | | | | | |
|---|---|---|---|---|---|
| 170 | 0.2249 | 0.000988 | 3.89E-07 | 1.89803E-05 | 0.967180744 |
| 180 | 0.26047 | 0.000819 | 3.27E-07 | 1.77059E-05 | 0.902239609 |
| 190 | 0.30087 | 0.000657 | 2.78E-07 | 1.59807E-05 | 0.814329091 |
| 200 | 0.34654 | 0.000512 | 2.39E-07 | 1.39861E-05 | 0.712691702 |
| 210 | 0.39699 | 0.000389 | 2.06E-07 | 1.18715E-05 | 0.60493738 |
| 220 | 0.45082 | 0.000288 | 1.79E-07 | 9.75613E-06 | 0.497143081 |
| 230 | 0.50608 | 0.000208 | 1.57E-07 | 7.74522E-06 | 0.394673383 |
| 240 | 0.56106 | 0.000147 | 1.38E-07 | 5.94065E-06 | 0.302717547 |
| 250 | 0.61494 | 0.000103 | 1.22E-07 | 4.46505E-06 | 0.227525846 |

**Table S5. Predictive model using 425 nm wavelength and 1.620 refractive index.**

| size | Ksc | I(theta) | c | K*I(theta)*c^(1/6) | normalized K*I*c^(1/6) |
|---|---|---|---|---|---|
| 10 | 4.79E-06 | 0.001852 | 0.00191 | 3.12645E-09 | 0.000173536 |
| 20 | 7.63E-05 | 0.001852 | 0.000239 | 3.51861E-08 | 0.001953037 |
| 30 | 0.000383 | 0.001851 | 7.07E-05 | 1.44108E-07 | 0.00799885 |
| 40 | 0.001194 | 0.00185 | 2.98E-05 | 3.89071E-07 | 0.021595785 |
| 50 | 0.002865 | 0.001847 | 1.53E-05 | 8.33442E-07 | 0.046261041 |
| 60 | 0.005807 | 0.001842 | 8.84E-06 | 1.53785E-06 | 0.085359663 |
| 70 | 0.010456 | 0.001833 | 5.57E-06 | 2.55164E-06 | 0.14163115 |
| 80 | 0.017221 | 0.001819 | 3.73E-06 | 3.90191E-06 | 0.216579453 |
| 90 | 0.026431 | 0.0018 | 2.62E-06 | 5.5849E-06 | 0.309995598 |
| 100 | 0.038282 | 0.001772 | 1.91E-06 | 7.55497E-06 | 0.419346041 |
| 110 | 0.052796 | 0.001733 | 1.43E-06 | 9.71945E-06 | 0.539487848 |
| 120 | 0.069809 | 0.001682 | 1.11E-06 | 1.19419E-05 | 0.662849352 |
| 130 | 0.089007 | 0.001615 | 8.69E-07 | 1.40462E-05 | 0.779648938 |
| 140 | 0.11002 | 0.00153 | 6.96E-07 | 1.58479E-05 | 0.879655927 |
| 150 | 0.13257 | 0.001425 | 5.66E-07 | 1.71824E-05 | 0.953728134 |
| 160 | 0.15656 | 0.0013 | 4.66E-07 | 1.79222E-05 | 0.994787109 |
| 170 | 0.18225 | 0.001157 | 3.89E-07 | 1.80161E-05 | 1 |
| 180 | 0.21021 | 0.001002 | 3.27E-07 | 1.74954E-05 | 0.971101049 |
| 190 | 0.24126 | 0.000843 | 2.78E-07 | 1.64427E-05 | 0.912668939 |
| 200 | 0.27617 | 0.00069 | 2.39E-07 | 1.50041E-05 | 0.832817989 |
| 210 | 0.31541 | 0.000549 | 2.06E-07 | 1.3308E-05 | 0.738675564 |
| 220 | 0.35884 | 0.000426 | 1.79E-07 | 1.14764E-05 | 0.637009507 |

| | | | | | |
|---|---|---|---|---|---|
| 230 | 0.40565 | 0.000323 | 1.57E-07 | 9.62067E-06 | 0.534005045 |
| 240 | 0.45447 | 0.000239 | 1.38E-07 | 7.81578E-06 | 0.433822776 |
| 250 | 0.50385 | 0.000173 | 1.22E-07 | 6.1456E-06 | 0.341117819 |

**Table S6. Predictive model using 450 nm wavelength and 1.613 refractive index.**

| size | Ksc | I(theta) | c | K*I(theta)*c^(1/6) | normalized K*I*c^(1/6) |
|---|---|---|---|---|---|
| 10 | 3.65E-06 | 0.001852 | 0.00191 | 2.3787E-09 | 0.00014219 |
| 20 | 5.81E-05 | 0.001852 | 0.000239 | 2.67831E-08 | 0.001600999 |
| 30 | 0.000292 | 0.001851 | 7.07E-05 | 1.09783E-07 | 0.006562422 |
| 40 | 0.000911 | 0.00185 | 2.98E-05 | 2.96814E-07 | 0.017742441 |
| 50 | 0.002189 | 0.001848 | 1.53E-05 | 6.37199E-07 | 0.038089444 |
| 60 | 0.004448 | 0.001844 | 8.84E-06 | 1.17926E-06 | 0.070491619 |
| 70 | 0.008035 | 0.001837 | 5.57E-06 | 1.96494E-06 | 0.117457177 |
| 80 | 0.013289 | 0.001826 | 3.73E-06 | 3.0225E-06 | 0.180674323 |
| 90 | 0.020507 | 0.001811 | 2.62E-06 | 4.35945E-06 | 0.260592181 |
| 100 | 0.029901 | 0.001789 | 1.91E-06 | 5.95722E-06 | 0.35610084 |
| 110 | 0.041565 | 0.001758 | 1.43E-06 | 7.76193E-06 | 0.463979773 |
| 120 | 0.055455 | 0.001718 | 1.11E-06 | 9.68936E-06 | 0.579194565 |
| 130 | 0.071394 | 0.001666 | 8.69E-07 | 1.16193E-05 | 0.694562153 |
| 140 | 0.089111 | 0.001599 | 6.96E-07 | 1.34124E-05 | 0.801745765 |
| 150 | 0.10831 | 0.001515 | 5.66E-07 | 1.49258E-05 | 0.892208358 |
| 160 | 0.12879 | 0.001414 | 4.66E-07 | 1.60341E-05 | 0.958462442 |
| 170 | 0.1505 | 0.001295 | 3.89E-07 | 1.66493E-05 | 0.995237254 |
| 180 | 0.17365 | 0.00116 | 3.27E-07 | 1.6729E-05 | 1 |
| 190 | 0.19869 | 0.001015 | 2.78E-07 | 1.62951E-05 | 0.974061931 |
| 200 | 0.22624 | 0.000865 | 2.39E-07 | 1.54158E-05 | 0.921502908 |
| 210 | 0.25694 | 0.000719 | 2.06E-07 | 1.41926E-05 | 0.848382948 |
| 220 | 0.29124 | 0.000582 | 1.79E-07 | 1.2732E-05 | 0.761069969 |
| 230 | 0.32918 | 0.000461 | 1.57E-07 | 1.11426E-05 | 0.666065958 |
| 240 | 0.37029 | 0.000357 | 1.38E-07 | 9.50208E-06 | 0.567999949 |
| 250 | 0.41366 | 0.00027 | 1.22E-07 | 7.8803E-06 | 0.471055579 |

## Error Analysis

**Table S7. Discrepancy between model prediction and experimentally determined $I/I_{max}$ values.**

| **absolute difference (nm)** | | | | | | |
|---|---|---|---|---|---|---|
| | **52 nm particle** | **101 nm particle** | **151 nm particle** | **206 nm particle** | average | net average |
| **375 nm** | 19.81638 | 9.668443429 | n/a | 13.82852 | **14.43778** | **6.503776882** |
| **400 nm** | 10.14687 | 5.185021212 | 1 | 1.992022 | **4.580979** | |
| **425 nm** | 10.03776 | 5.610918155 | 1 | 0.707205 | **4.33897** | |
| **450 nm** | 9.875392 | 5.379012185 | 1 | 2.30911 | **4.640879** | |
| average | **12.4691** | **6.460848745** | **1** | **4.709215** | | |
| **% difference** | | | | | average | net average |
| **375 nm** | 38.10842 | 9.572716267 | n/a | 6.712876 | **18.13134** | **8.842302044** |
| **400 nm** | 19.51321 | 5.133684368 | 0.662252 | 0.967001 | **6.569038** | |
| **425 nm** | 19.30338 | 5.55536451 | 0.662252 | 0.343303 | **6.466074** | |
| **450 nm** | 18.99114 | 5.325754638 | 0.662252 | 1.120927 | **6.525018** | |
| average | **23.97904** | **6.396879946** | **0.662252** | **2.286027** | | |

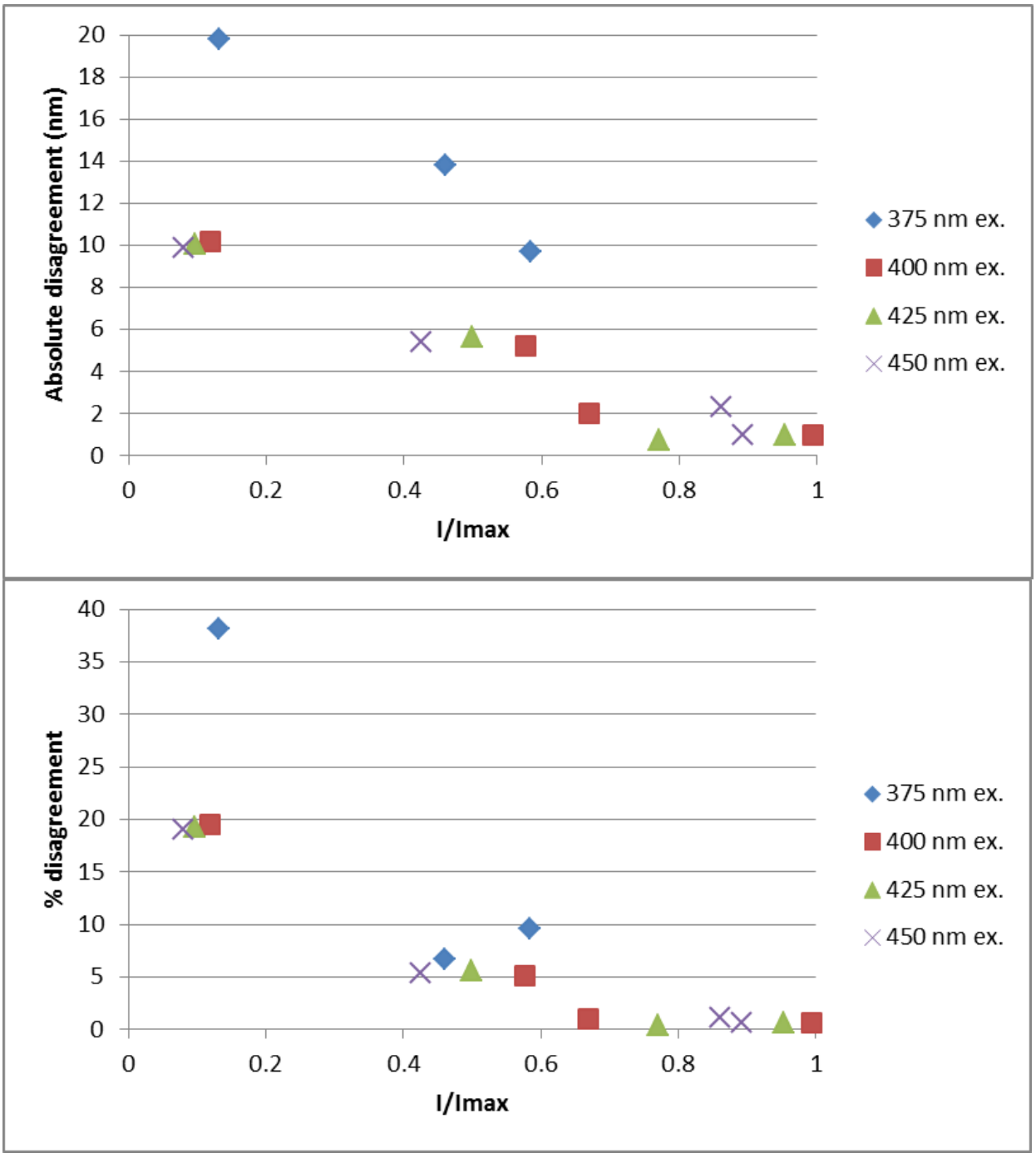


Figure S8. Agreement between model and experiment improves with increasing $I/I_{max}$.